



NAVAL MEDICAL RESEARCH UNIT SAN ANTONIO

**Gold Nanoparticle-assisted Laser Therapy for the Disruption of
Methicillin-resistant *Staphylococcus aureus* Biofilms**

DICKSON KIRUI, PH.D.
TAREA BURTON, M.S.
GREGOR WEBER, PH.D.
NANCY MILLENBAUGH, PH.D.

MAXILLOFACIAL INJURY AND DISEASE DEPARTMENT
CRANIOFACIAL HEALTH AND RESTORATIVE MEDICINE DIRECTORATE

NAMRU-SA REPORT # 2017-16

Approved for public release; distribution is unlimited

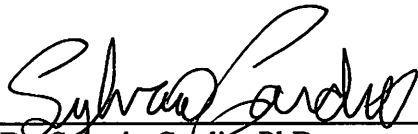
DECLARATION OF INTEREST

The views expressed in this article are those of the authors and do not necessarily reflect the official policy or position of the Department of the Navy, Department of Defense, nor the U.S. Government. Authors are employees or contractors of the U.S. Government. This work was prepared as part of their official duties. Title 17 USC §105 provides that 'copyright protection under this title is not available for any work of the U.S. Government.' Title 17 USC §101 defines a U.S. Government work as a work prepared by a military service member or employee of the U.S. Government as part of that person's official duties.

ACKNOWLEDGEMENTS

The authors gratefully acknowledge Mr. Duane Cox (NAMRU-SA) for fabricating plate holders used in the automated gantry, Ms. Bridget Endler and Mr. Roy Dory (NAMRU-SA) for programming software used for gantry automation, and Mr. Joel Bixler (U.S. Air Force, JBSA-Fort Sam Houston, TX) for assistance in laser beam alignment and laser dosimetry analyses. This work was funded by Naval Medical Research Center's Advanced Medical Development Program using work unit number G1025. This research was supported in part by an appointment to the Postgraduate Research Participation Program at NAMRU-SA administered by the Oak Ridge Institute for Science and Education through an interagency agreement between the U.S. Department of Energy and NAMRU-SA.

REVIEWED AND APPROVED BY:



Dr. Sylvain Cardin, PhD
Chief Science Director
Chair, Scientific Review Board
Naval Medical Research Unit San Antonio
3650 Chambers Pass, BLDG 3610
Fort Sam Houston, TX 78234-6315

12/7/16
Date



CAPT Montcalm-Smith, MSC, USN
Commanding Officer
Naval Medical Research Unit San Antonio
3650 Chambers Pass, BLDG 3610
Fort Sam Houston, TX 78234-6315

12/8/2016
Date

TABLE OF CONTENTS

ABBREVIATIONS	4
1. EXECUTIVE SUMMARY	5
2. INTRODUCTION	6
3. MATERIALS AND METHODS	8
4. RESULTS AND DISCUSSION.....	12
5. CONCLUSION AND FUTURE DIRECTION	16
6. MILITARY SIGNIFICANCE	17
7. FIGURES	18
8. REFERENCES	24

ABBREVIATIONS

CFU	Colony forming unit
CLSM	Confocal laser scanning microscopy
Con-A	Concanavalin-A-Alexa Fluor® 488
CV	Crystal violet
DAPI	4, 6-diamidino-2-phenylindole
EPS	Exopolysaccharide
FOV	Field of view
GNPs	Gold nanoparticles
MDR	Multi-drug resistant
MRSA	Methicillin-resistant <i>Staphylococcus aureus</i>
Nd:YAG	Neodymium-doped yttrium-aluminum-garnet
PBS	Phosphate-buffered saline
SD	Standard deviation
SPR	Surface plasmon resonance
TSA	Tryptic soy agar
TSB	Tryptic soy broth

1. EXECUTIVE SUMMARY

Objective: Effective treatment of combat-related maxillofacial infections is hindered by the ability of bacterial pathogens to produce biofilms containing a dense exopolysaccharide (EPS) matrix. The EPS matrix protects microorganisms against the host immune system, blocks delivery of antibiotics, and often leads to drug tolerance. In recent years, there has been increased interest in developing alternative treatment strategies that can improve efficacy of mainstay antibiotic regimens by disrupting the EPS matrix. One attractive approach is to use pulsed laser irradiation to rapidly damage the EPS matrix with nanosecond opto-acoustic waves and high temperatures. Here, we optimize and successfully demonstrate the use of gold nanoparticle (GNP)-assisted pulsed laser therapy to disperse *in vitro* methicillin-resistant *Staphylococcus aureus* (MRSA) biofilms.

Methods: Overnight cultures of MRSA were suspended at $\sim 10^7$ colony forming units (CFUs)/mL in tryptic soy broth supplemented with 10% human plasma and grown in fibrinogen-coated glass-bottom 96-well microplates at 37°C under static conditions. Biofilms were pre-treated with 0, 62.5, 125, 250, or 500 $\mu\text{g/mL}$ of GNPs for 1–5 h and then treated with pulsed laser irradiation (532 nm, 8 ns, 1 Hz) ranging from 10–110 pulses. The crystal violet (CV) assay was used to visualize the integrity of the biofilms and quantify alterations in the biomass after treatment. Confocal microscopy was used to assess the extent of biofilm damage, while CFU assays were used to evaluate the level of bacterial colony dispersal.

Results: CV assays revealed optimal dispersion of MRSA biofilms after incubation with 500 $\mu\text{g/mL}$ of GNPs for 5 h and treatment with 50 laser pulses. Treatment of the biofilms with a combination of GNPs and laser irradiation led to a $63 \pm 8\%$ reduction in CFUs relative to controls. The treatment also led to $79 \pm 10\%$ dispersion of biofilms as evidenced by confocal microscopy. Conversely, biofilms treated with 50 laser pulses alone or GNPs alone remained robust with no discernible dispersion or reduction in CFUs compared to untreated controls.

Conclusion: These results demonstrate the use of GNP-assisted laser therapy as a potential strategy to physically destroy biofilms, and thus eradicate a protective barrier surrounding persistent wound pathogens. This approach could improve delivery of antibiotics to the remaining bacterial cells and enhance therapeutic efficacy of mainstay treatment regimens. Future studies will investigate the use of targeting agents to selectively destroy MRSA infections while reducing collateral damage to healthy tissue.

2. INTRODUCTION

Multi-drug resistant (MDR) pathogens are becoming the most common cause of infectious disease-related deaths around the world, killing more Americans every year than colon and breast cancer combined [1]. The escalating emergence of MDR pathogens has been attributed as a primary cause of illness in 2 million patients, resulting in 23,000 mortalities annually in the U.S. [2]. Complications due to ineffective treatment of underlying drug-resistant infections have been associated with 75% of deaths from burn-related wounds [3], and treatment of infection-related illnesses now costs the U.S. healthcare system an estimated \$20–35 billion per year [4, 5]. Furthermore, infections caused by MDR bacterial strains, which comprise 15–53% of isolates in military hospitals [6, 7], complicate the treatment and recovery of combat-injured U.S. military personnel and adversely impact battlefield readiness. Likewise, MDR strains comprise ~50% of all isolates in the civilian population [8].

In addition to genetically-based resistance mechanisms, MDR pathogens commonly exhibit increased drug tolerance due to formation of biofilms [9], which have been shown to be 500–5,000-fold less susceptible to antibiotics than planktonic cells [10]. Biofilms are complex, often multi-species microbial communities that are enclosed in an exopolysaccharide (EPS) matrix and attached to a surface [11]. The dense EPS matrix acts as a barrier to antimicrobial agents by limiting antibiotic penetration into the biofilm [12] and absorbing and binding the antibiotic within the biofilm extracellular matrix [13, 14]. This is illustrated in **Figure 1**, which shows representative confocal micrographs of *Staphylococcus aureus* biofilms with dense EPS matrices that have trapped and significantly hindered penetration of macromolecules into the biofilm. The biofilm matrix also creates a milieu that enhances the expression of genes involved in drug tolerance and induces cellular dormancy [13, 14]. Many antibiotics used to treat chronic wounds are poorly effective against quiescent cells because these agents were developed to target exponentially growing microorganisms. The result is that, even at high antibiotic concentrations and despite prolonged treatments, a subset of bacteria within biofilms persist and cause recurrent infections [15]. This is a major concern because 65–80% of all infections are reported to be biofilm-related [16], and no biofilm-specific treatments are currently available for use in the clinical setting.

Given this escalating medical crisis, research efforts have increased to discover alternative treatments for both planktonic and biofilm infections that are less likely to cause drug resistance

[17-19]. These approaches include the use of mechanical methods/external stimuli, such as thermal therapy [18] and photo-acoustic waves [20] produced by focused laser irradiation, to disperse biofilms and destroy bacterial colonies [21, 22]. The heat and physical pressure generated by the laser disrupts critical biochemical processes, damages cell walls and membranes, causes cellular disintegration, and decreases bacterial viability [17, 19, 21]. Laser therapy has been widely used for decades to treat various ailments such as rheumatoid arthritis [23], cancer [24, 25], and infections [26]. However, a major drawback is the collateral, non-specific damage caused by the use of high-energy laser therapy resulting in extensive injury to healthy tissue. Fortunately, recent advances in nanotechnology and functionalization chemistry have led to the development of novel nanomaterials that can mediate, localize, and enhance thermal treatment while mitigating non-selective damage to healthy tissue [27]. Particularly, gold nanoparticles (GNPs) are unique materials that possess strong surface plasmon resonance (SPR) properties in which the particles strongly absorb energy in the visible region and release the energy to the surrounding area (medium or cells) through phonon-phonon interactions [28]. This SPR phenomenon can lead to a dramatic enhancement (up to 10^6) in generated thermal energy compared to conventional energy-absorbing dyes [29, 30], making GNPs ideal materials to convert externally applied low-energy laser irradiation into highly-destructive thermal energy localized to diseased regions [31]. Additionally, these types of materials can convert absorbed photons into thermal energy in the picosecond time scale, causing rapid cell destruction [32]. Various types of gold nanostructures, including spherical nanoparticles [19] and nanorods [21], and other heat-generating particles, such as single-walled carbon nanotubes [33], have been tested as thermally-inducing antimicrobial agents.

The use of laser therapy to kill bacteria or to enhance the bactericidal activity of conventional antibiotics has been previously reported in the literature [21, 33-36]. Using planktonic cultures, several groups have demonstrated the potency of laser therapy against many different strains of bacterial pathogens [17, 19, 21], whereby 40-nm GNPs are commonly used in combination with laser irradiation in the visible range (420–570 nm) [30]. However, a glaring deficiency in these prior studies is the limited investigation into the therapeutic potential of laser therapy against bacterial biofilms, which more closely approximate conditions in clinical wounds. In this work, we evaluated the efficacy of GNP-assisted laser therapy to disperse biofilms of methicillin-resistant *Staphylococcus aureus* (MRSA). This opportunistic pathogen was selected because it is

known to produce biofilms [37], is one of the leading causes of infections in surgical and burn wounds associated with combat-related injuries in U.S. military personnel [38], and is difficult to treat [39].

3. MATERIALS AND METHODS

3.1 Reagents and materials

GNPs (Cat. No. CS11-40) were purchased from Nanopartz, Inc. (Loveland, CO). Concanavalin-A-Alexa Fluor® 488 (Con-A), 4',6-diamidino-2-phenylindole (DAPI), ProLong® Gold antifade reagent and phosphate-buffered saline (PBS) were purchased from Life Technologies (Carlsbad, CA). Polystyrene plates and reagents used to make tryptic soy broth (TSB) and tryptic soy agar (TSA) were purchased from Fisher Scientific (Hanover Park, IL). Human plasma was obtained from Biological Specialty Corporation (Colmar, PA). Corning® 96-well glass-bottom microtiter plates, crystal violet (CV) dye, human fibrinogen, and all other reagents were purchased from Sigma-Aldrich (St. Louis, MO).

3.2 Bacterial strain and biofilm preparation

MRSA derived from a clinical wound isolate (SA5120) was obtained from a cell repository at the U.S. Army Institute of Surgical Research on JBSA-Fort Sam Houston (San Antonio, TX). Bacterial stocks were maintained at -80°C, and colonies were grown overnight by streaking onto TSA plates. An inoculum was then prepared in TSB and grown for 18 h at 37°C on a shaker at 250 rpm. The bacterial inoculum was diluted to obtain an optical density at 600 nm (OD₆₀₀) of 0.1, which is equivalent to $\sim 10^7$ colony forming units (CFU)/mL, using TSB supplemented with 10% human plasma. Bacterial suspensions (100 μ L) were added to 96-well glass-bottom culture plates that had been pre-treated with 1 mg/mL of fibrinogen and then cultured for biofilm formation for 24 h at 37°C under static conditions. The media was then gently aspirated from the wells and the biofilms were gently rinsed once with PBS to remove non-adherent cells. The biofilms were subsequently utilized to evaluate the effects of GNP-assisted laser therapy and were analyzed using CV staining, CFU assays, and confocal laser scanning microscopy (CLSM).

3.3 Preparation of GNP working solution

GNPs (diameter = 40 nm) were provided by the manufacturer at a concentration of 7.5×10^{12} GNPs/mL, or 4.3 mg/mL, in a buffered solution. Working concentrations of GNPs at 62.5–500 µg/mL were prepared in 20 mM Tris-HCl with 100 mM NaCl buffer at pH 7.4.

3.4. GNP-assisted laser therapy

A pulsed neodymium-doped yttrium-aluminum-garnet (Nd:YAG) laser manufactured by Big Sky Laser/Quantel (Bozeman, MT) was used for therapy. The laser provides 8-ns pulses at 532 nm with a 1 Hz repetition rate. The exposure system is also equipped with an XY-gantry system controlled with LabVIEW software (National Instruments, Austin, TX) that allows automatic positioning of biofilm samples and activation of the laser. This ensured highly accurate alignment of the samples with the laser beam and reduced variability in the laser dosimetry. The laser beam was focused on the surface of the samples using a plano-convex spherical lens with a 25.4-mm focal length (ThorLabs, Inc., Austin, TX). ZAP-IT[®] Laser Alignment Paper (Zap-It Corporation, Salisbury, NH) was used to estimate the approximate size of the beam and confirm alignment of the beam with the sample. The size of the laser beam was altered by adjusting the spacing between the sample and the focal lens, whereby a ~4.4-mm laser beam was obtained by placing a 96-well microtiter plate (4.5-mm well diameter) 94 mm away from the focal lens. This configuration allowed irradiation of ~95% of the area in the bottom of the well at a fluence of ~1.3 J/cm². Laser dosimetry readings were collected before and after each experimental run using an Ophir power meter and detector (Ophir Photonics Groups, North Logan, UT) mounted on the table below the sample holder.

Prior to treatment, the laser system was pre-warmed for at least 30 min to ensure stable laser output. Biofilms were pre-incubated with GNPs, the GNP solution was removed, and then 40 µL of 20 mM Tris-HCl with 100 mM NaCl buffer was added to the wells. Each sample was treated with a pre-programmed number of pulses (10–110 pulses) or sham exposed using the automated exposure system. Samples exposed to vehicle only or laser alone without GNPs were included as controls.

3.5 Assessment of GNP-assisted laser therapy effects using the CV assay

The effect of GNP-assisted laser treatment was evaluated using a colorimetric CV assay that measures total biofilm biomass (cells and extracellular matrix). After treatment, the buffer was aspirated from the sample wells and the biofilms were rinsed once with PBS. A 0.01% CV working solution was then added to each well, and samples were incubated for 30 min at room temperature. The dye solution was aspirated from each well, and biofilms were rinsed twice using PBS. The plates were incubated at room temperature for 30 min to allow the wells to dry before the addition of 100 μ L of 95% ethanol. The samples were further incubated for 30 min to solubilize the dye. The absorbance of the CV dye was measured at 595 nm (OD_{595}) using a BioTek Synergy HT plate reader with Gen5 software (version 2.0, BioTek, Winooski, VT).

3.6 Assessment of GNP-assisted laser therapy-induced biofilm dispersal using the CFU assay

The efficacy of GNP-assisted laser therapy in dispersing bacterial colonies from the biofilms was evaluated using the CFU assay. Upon completion of sample treatments, the buffer was removed from the biofilms and the wells were gently washed once with PBS. Papain treatment was then performed to loosen and disperse the remaining biofilm, and thus help ensure complete release of cells from the wells. To accomplish this, the biofilms were treated with 40 μ L of papain at 100 μ g/mL for 30 min at 37°C under static conditions. The papain wash was collected in microfuge tubes, centrifuged for 10 min at 4,000 rcf to pellet the cells, and then re-suspended in 100 μ L of PBS. The biofilms remaining in the wells were re-suspended in 100 μ L of PBS by repeated pipetting and transferred into microfuge tubes, which were then sonicated for 30 sec to further break up the biofilms. Cells recovered in the papain wash and the sonicated fractions were serially diluted in PBS and then streaked onto TSA plates. Bacterial colonies on the TSA plates were allowed to grow overnight in a 37°C incubator and the number of colonies were enumerated and expressed as CFUs/mL. The data from these assays are presented as the sum of the colony counts obtained from the papain wash and the sonicated fraction. Pilot experiments confirmed that treatment of planktonic SA5120 cultures with 100 μ g/mL of papain for up to 24 h at 37°C did not decrease bacterial viability (data not shown).

3.7 Assessment of GNP-assisted laser therapy using CLSM

CLSM was used to visually assess the level of biofilm dispersal. After treatment, buffer was aspirated and biofilms were washed once with PBS and then incubated with 50 mM Con-A for 30 min at room temperature. Thereafter, Con-A supernatant was aspirated from the wells, samples were incubated with 100 μ L of DAPI at 0.5 μ g/mL for 5 min, and the wells were washed with PBS. Con-A (green) stains the EPS while DAPI (blue) labels the nucleic acid components of the biofilm, including bacterial cells. ProLong[®] Gold antifade reagent (20 μ L) was added to minimize photobleaching and to preserve the fluorescent signal. The samples were subsequently imaged using a Nikon Eclipse C1 confocal laser scanning microscope (Nikon, Melville, NY). Fluorescent signals were acquired using the following settings: excitation at 405 nm with a band-pass emission filter centered at 430 nm for DAPI and excitation at 488 nm and a band-pass filter centered at 525 nm for Con-A. Two-channel images (green and blue) of MRSA biofilms were acquired over multiple fields of view (FOVs) using a 20 \times objective lens. To minimize local photobleaching and account for biofilm heterogeneity, five non-overlapping FOVs were selected and imaged for each biofilm sample. For samples exposed to GNPs in combination with laser irradiation, a distinct central zone of biofilm damage surrounded by an outer zone with less damage was observed. This damage pattern was most likely due to the Gaussian distribution of energy in the laser beam and use of a laser beam with a slightly smaller diameter than that of the sample wells, i.e., 4.4 mm versus 4.5 mm, respectively. The five FOVs, therefore, were randomly selected from the central zone of damage in these samples. Samples in the other treatment groups did not exhibit these two distinct zones of damage, and thus images were acquired from randomly selected FOVs in the central portion of the wells.

3.8 Image analysis

The extent of biofilm damage was evaluated using ImageJ[®] image analysis software (NIH, Bethesda, MD) to estimate the amount of biofilm present in the confocal microscopy images, accounting for both extracellular matrix and cellular components. This was calculated based on the intensity of Con-A and DAPI fluorescent signals in the non-overlapping FOVs ($n = 5$ /biofilm sample). Fluorescent intensity in the selected FOVs was measured using the “threshold” function where fluorescence was defined by setting low and high pixel thresholds to include visible green and blue signals and exclude single background noise pixels. The settings were applied to all

images and the “analyze particles” function was used to generate total area fraction containing Con-A and DAPI, i.e., percent of pixels in the image that fell within the low and high pixel thresholds. The resulting area fraction data, which represents the fraction of the surface area covered by biofilm, were expressed as a percentage of the controls and reported as “substratum coverage” in the results.

3.9 Statistics

Data are presented as the mean \pm standard deviation (SD). GraphPad Prism software (version 6.07, GraphPad Software, Inc., La Jolla, CA) was used to determine statistical significance, in which one-way ANOVA and post hoc Tukey multiple comparison tests were utilized to compare differences between treatment groups. A value of $p < 0.05$ was considered statistically significant.

4. RESULTS AND DISCUSSION

4.1 Laser therapy exposure system

The laser exposure system, which includes an Nd:YAG 8-ns pulsed laser, was configured to allow optimal irradiation of biofilms grown in 96-well microtiter plates and reduce potentially harmful stray laser radiation. **Figure 2A** depicts the laser set-up, which consists of a laser head and an XY gantry system programmed with LabVIEW software to allow automated operation. The laser head was mounted vertically to directly radiate the biofilm samples placed on the XY gantry system. This orientation also reduces the potential exposure to stray beams compared to use of a laser head mounted horizontally with a collimating laser mirror to redirect the beam path at a 90° angle into the sample. A plano-convex spherical lens was used to focus the beam and alter its size by adjusting the spacing between the lens and the XY gantry system (**Figure 2A**). The 4.4-mm laser beam irradiated the microtiter plate resulting in a laser fluence of $\sim 1.3 \text{ J/cm}^2$ (**Figure 2B**). The reproducibility of the laser output and alignment of the sample plate with the laser beam by the automated gantry system were assessed by evaluating the well-to-well, intra-day, and inter-day variability in laser pulse energy. The overall mean \pm SD of laser output measured before and after every experimental run was $202.7 \pm 2.8 \text{ mJ/pulse}$, with daily averages of 197.5–207.1 mJ/pulse and intra-day SDs of $\leq 2.2 \text{ mJ/pulse}$. Over a range of varying number of pulses delivered to different wells of an empty 96-well microtiter plate, the mean \pm SD of

laser energy measured after the beam passed through the plate was 180.6 ± 1.4 mJ/pulse (**Figure 2C**). Furthermore, the day-to-day level of ‘pass through’ laser energy was stable with an average \pm SD of 181.7 ± 2.6 mJ/pulse over the course of 43 days (**Figure 2D**). Intra-day variations in the ‘pass through’ laser energy were small (SDs of ≤ 3.0 mJ/pulse), as evidenced by the consistent energy readings recorded at the beginning and end of individual experimental runs (**Figure 2D**). The low SDs in the dosimetry data confirmed that the laser output was stable and alignment of the sample with the laser beam by the automated gantry system was consistently accurate and precise.

4.2 Optimal laser dosage required to destroy MRSA biofilms

Previous work in our laboratory showed that use of $\sim 7 \times 10^{10}$ GNPs/mL in combination with 100 laser pulses caused significant reduction in the viability of planktonic *S. aureus* cultures [17]. Using these treatment conditions as a guide, laser therapy parameters that affect biofilm destruction, including the laser dosage (number of laser pulses), duration of particle incubation with the biofilm, and concentration of GNPs were optimized in a series of experiments to ensure effective therapy while reducing unnecessarily high laser doses that could damage normal host tissue.

To optimize laser dosage, an experiment was conducted to first determine the effect of laser irradiation alone (no GNPs) on biofilms. The goal of this testing was to identify a range of number of pulses that would cause little to no significant damage to the biofilms, and therefore, be safer for host tissues. **Figure 3A** shows CV assay results from biofilms irradiated with 0 to 110 laser pulses. Treatment of biofilms with 80 or 110 laser pulses resulted in significant reduction in biofilm biomass compared to controls, whereas 30 pulses did not cause a significant decrease in biofilm biomass. These results indicate the threshold for induction of biofilm damage by laser exposure alone was less than 80 pulses.

The amount of laser energy needed to degrade biofilms in combination with GNPs was then determined by varying the number of pulses delivered to the biofilm sample from 0 to 50, while keeping the concentration of GNPs constant at 62.5 μ g/mL ($\sim 1 \times 10^{11}$ GNPs/mL). The aim was to determine the lower threshold of laser energy that could disperse *S. aureus* biofilms when combined with the GNPs. **Figure 3B** shows the CV assay of biofilm biomass in samples after treatment. The findings revealed that treatment with less than 50 pulses of laser irradiation, even

when combined with GNP treatment, did not cause significant damage to biofilms. It was only when biofilms were pre-treated with GNPs and irradiated with 50 laser pulses that a significant reduction in the amount of biofilm was observed. In contrast, treatment with 50 pulses of laser alone did not significantly damage the biofilms, suggesting that this laser dosage would be optimal for use with GNPs to enhance therapy. It was also noted that treatment of biofilms with GNPs alone at 62.5 $\mu\text{g/mL}$ did not cause significant reduction in biofilm biomass compared to controls. Taken together, these results show that GNPs enhance the effect of the laser treatment, suggesting that GNP-assisted laser therapy may be an effective strategy to degrade biofilms.

4.3 Duration of nanoparticle incubation needed to achieve optimal GNP-assisted laser therapy-induced biofilm damage

The duration of GNP incubation with biofilms prior to laser irradiation was varied, while keeping GNP concentration and laser dosage constant, to determine the incubation time-point that provides maximal laser therapy effect. The number of laser pulses was set to 50, based upon results from the previous experiments described above. The GNP concentration, however, was increased to 125 $\mu\text{g/mL}$ in this experiment to determine if this increase would enhance biofilm destruction compared to that observed in the previous set of experiments. Biofilms were pre-treated with GNPs for durations ranging from 1 to 5 h, irradiated with 50 laser pulses, and then evaluated using the CV assay. **Figure 4** shows images of biofilms stained with CV dye and the corresponding absorbance measurements. The group pre-treated with GNPs for 5 h exhibited the highest level of biofilm degradation (dark areas in the center of the wells) compared to samples pre-treated with particles for shorter durations (i.e., 1, 2, 3, or 4 h) (**Figure 4A**). Consistent with this data, the CV dye absorbance measurements revealed a significant reduction in biomass for the 5-h incubation time-point, suggesting that this duration is required for sufficient attachment of GNPs to the biofilm (**Figure 4B**). Also, treatment of biofilms with GNPs alone at 125 $\mu\text{g/mL}$ did not cause a reduction in biofilm biomass compared to controls, indicating this concentration could be included in subsequent experiments involving optimization of GNP concentration.

Laser dosimetry data collected after the beam passed through the biofilms and exited the bottom of the sample plate are shown in **Figure 4C**. It was notable that the amount of laser energy exiting the samples was markedly reduced for the 5-h incubation group compared to the other experimental groups (**Figure 4C**). The reduced pass through energy indicates more of the

incident laser energy was absorbed due to a greater number of GNPs attached to the biofilms after 5 h of incubation. Taken together, the findings indicate that 5 h was an optimal duration for GNP incubation because it allowed sufficient attachment of particles to biofilms, thereby enhancing the effect of laser therapy.

4.4 Optimization of GNP concentration for GNP-assisted laser therapy-induced destruction of biofilms

Thus far, CV assay results indicated that GNP-assisted laser therapy could significantly reduce total biofilm biomass (extracellular matrix and bacterial cells). The next phase of testing focused on using CFU assays to evaluate more specifically the level of bacterial colony dispersion from biofilms induced by GNP-assisted laser therapy and to further optimize GNP concentration. The number of laser pulses was kept constant at 50, as in the previous experiment, and GNP concentrations of 125 and 500 µg/mL were tested to determine if increasing the GNP concentration would enhance dispersion of bacteria from the biofilms. After completion of laser therapy, cells were extracted from biofilms, serially diluted, and plated onto TSA plates to obtain colony counts for calculation of CFUs/mL.

Figure 5 summarizes the results obtained from three independent CFU experiments. The untreated control was shown to form robust MRSA biofilms with an average of 1.4×10^8 viable cells/biofilm. Biofilms treated with 50 pulses of laser alone or with GNPs alone at 125 µg/mL (G125) or 500 µg/mL (G500) showed no significant cell dispersion compared to controls. In contrast to findings from the previous experiment in which the CV assay was used (**Figure 4**), the CFU assays showed that treatment of biofilms with G125 plus laser irradiation did not induce significant bacterial colony dispersal. The reason for the lack of agreement in the results from the two assays is most likely due to differences in how samples are processed for the two assays, specifically, the greater number of washes used during the CV assay may have loosened more of the biofilm. Notably, the combination of G500 plus laser irradiation led to a $63 \pm 8\%$ dispersion of MRSA cells relative to the control (**Figure 5**). These findings demonstrated that combination therapy of G500 plus 50 laser pulses could significantly disperse MRSA colonies from biofilms.

4.5 Confocal microscopy confirmed that GNP-assisted laser therapy degraded MRSA biofilms

Confocal microscopy and image analysis were used to assess the extent of biofilm dispersion resulting from GNPs alone, laser treatment alone, and the combination of GNPs plus laser irradiation. Biofilms were incubated with 0, 125, 250, or 500 $\mu\text{g/mL}$ of GNPs for 5 h, irradiated with 50 pulses of laser, stained with Con-A and DAPI, and then imaged. **Figure 6** shows representative micrographs of biofilms (**Figure 6A**) and the image analysis results (**Figure 6B**) from three independent experiments. The images revealed that robust and dense biofilms formed after 24 h of growth as shown in the untreated control group (**Figure 6A**). When the biofilms were treated with 50 pulses of laser alone, no damage was observed. Likewise, biofilms treated with 125, 250, or 500 $\mu\text{g/mL}$ of GNPs (G125, G250, or G500) alone showed no evidence of dispersion, suggesting that neither laser irradiation alone nor GNPs alone caused any degradation of the samples (**Figure 6A**). The combination treatment of G125 followed by laser therapy resulted in a slight degradation of the biofilms (red arrows in **Figure 6A**). However, the combination treatment of G250 or G500 followed by laser therapy resulted in obvious dispersion of the *S. aureus* biofilms (**Figure 6A**).

Figure 6B shows the extent of biofilm damage in the acquired confocal micrographs quantified using ImageJ[®] analysis software. The findings confirmed that the combination treatment of G250 plus laser exposure led to significant biofilm dispersion, resulting in removal of $58 \pm 10\%$ of the MRSA biofilms. More significantly, the use of G500 plus laser irradiation proved to be the most effective biofilm dispersion strategy, resulting in removal of $79 \pm 10\%$ of the biofilms. The data also confirmed that treatment of biofilms with GNPs alone or laser irradiation alone caused no significant biofilm dispersion compared to controls. These findings demonstrate the effectiveness of GNP-assisted laser therapy for dispersion of biofilms and that laser treatment alone or GNPs alone is ineffective at causing significant degradation of the biofilms.

5. CONCLUSION AND FUTURE DIRECTION

GNP-assisted laser therapy caused significant dispersion of MRSA biofilms as evidenced by a 63% reduction in bacterial colony counts and a 79% reduction in surface area covered by the biofilms when visualized by confocal microscopy imaging. The use of optimized parameters, namely, pre-incubating biofilms with 500 $\mu\text{g/mL}$ of GNPs for 5 h followed by irradiation of

biofilms with 50 pulses of laser (8-ns, 532 nm), led to the highest dispersion of biofilms. The use of nanoparticle-assisted laser therapy, therefore, may be an effective means of eradicating biofilms and a promising strategy to improve treatment of bacterial infections. Future studies will investigate ways to incorporate targeting moieties onto the GNPs for selective attachment to the biofilms, use of GNP-assisted laser therapy in combination with traditional antibiotics, and the potential for use of GNP-assisted laser therapy as a novel standard of care for maxillofacial wound treatment.

6. MILITARY SIGNIFICANCE

Bacterial wound infections are problematic for the U.S. military around the globe, and can result in significant morbidity, long recovery periods, and high treatment costs for personnel with combat-related injuries. Antibiotic resistance and biofilm production have been associated with persistent infections in wounded military personnel [40]. Treatment strategies that are effective against MDR pathogens, have a low risk of inducing additional antibiotic resistance, and are active against biofilm infections are urgently needed. The data presented here provide important information on optimization and successful demonstration of a laser-based therapeutic approach for dispersing biofilms formed by a clinical MRSA strain. This research provides the framework for the further design and development of a novel strategy to remove biofilms, potentially enhance the efficacy of conventional antibiotic regimens, and ultimately improve battlefield readiness.

7. FIGURES

Figure 1

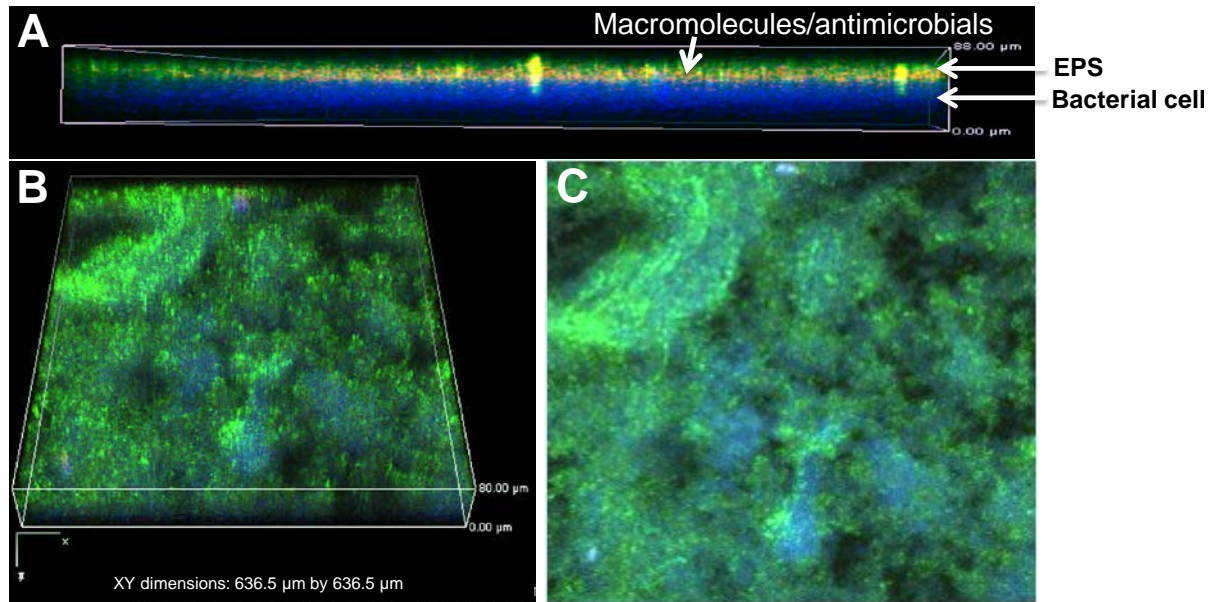


Figure 1: Confocal microscopy images of MRSA biofilms illustrating challenges posed by the dense EPS matrix, which include hindrance of penetration of conventional antimicrobials. MRSA biofilms were grown for 24 h then stained with Con-A to visualize polysaccharides (green) and DAPI to visualize nucleic acids (blue). A) Image illustrating the barrier effect of biofilms that limits the penetration of drug molecules (red) through the EPS matrix (green) and into the vicinity of the bacterial cells (blue). Co-localization of EPS matrix (green) and drug molecules (red) appear yellow. B) 3-D image of a mature biofilm; C) 2-D image of a mature biofilm showing the EPS matrix (green) surrounding bacterial cells (blue).

Figure 2

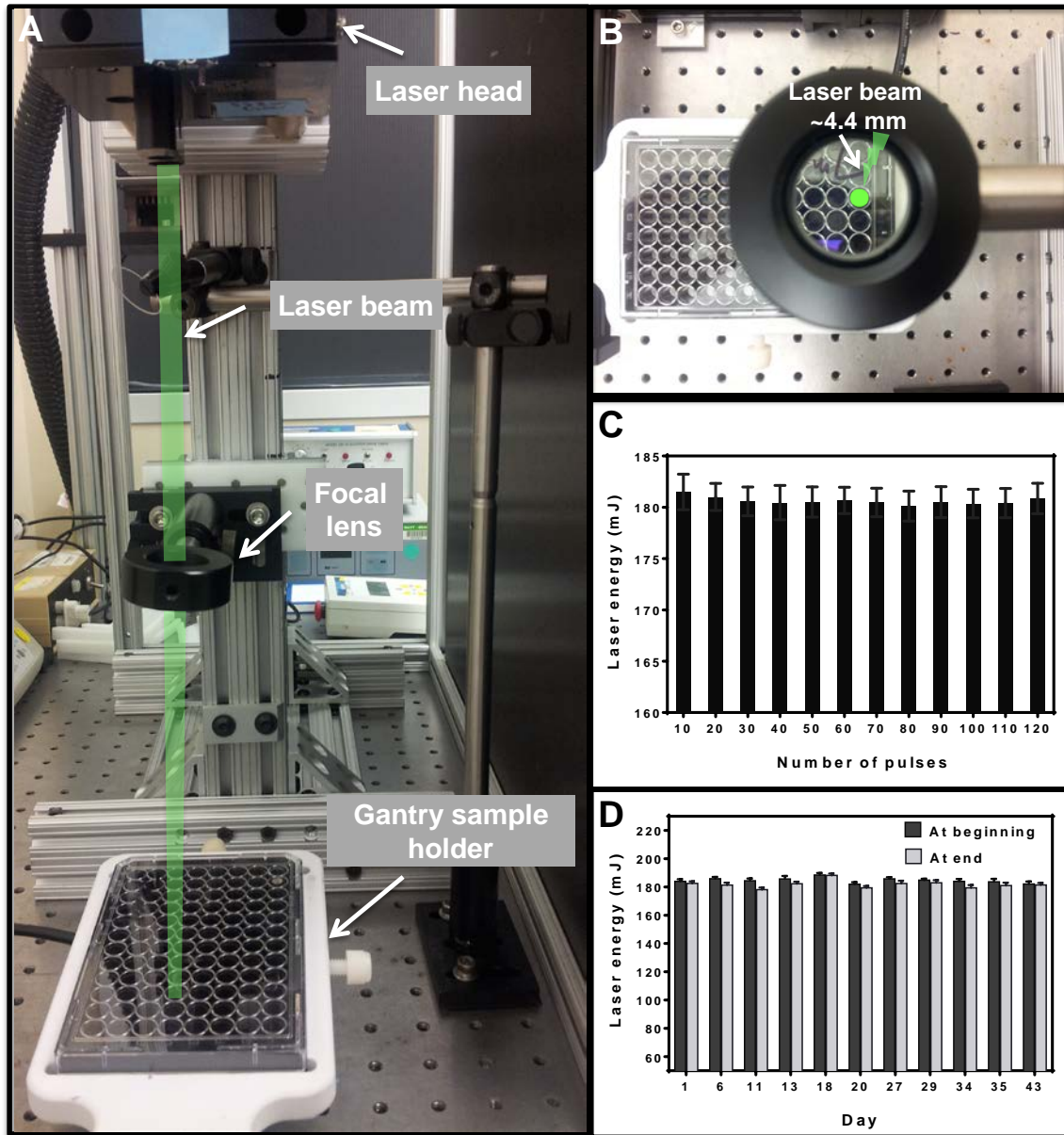


Figure 2: The laser exposure system configuration and dosimetry graphs showing consistent and stable laser pulse energy output. A) Image showing the laser head, focal lens, and XY gantry sample holder that enables automated sample alignment with the laser beam. B) Aerial view of sample wells seen through the focal lens. C) Power meter readings of laser pulse energy after passing through an empty sample plate for varying numbers of pulses delivered to different wells of the plate. Data are shown as the mean \pm SD and show stable levels of laser energy with an overall mean \pm SD of 180.6 ± 1.4 mJ. D) The level of pass through laser pulse energy was stable at 181.7 ± 2.6 mJ over the course of 43 days of operation with ≤ 3.0 mJ of intra-day variability. Data are shown as the mean \pm SD of $n = 5$ laser pulses per well.

Figure 3

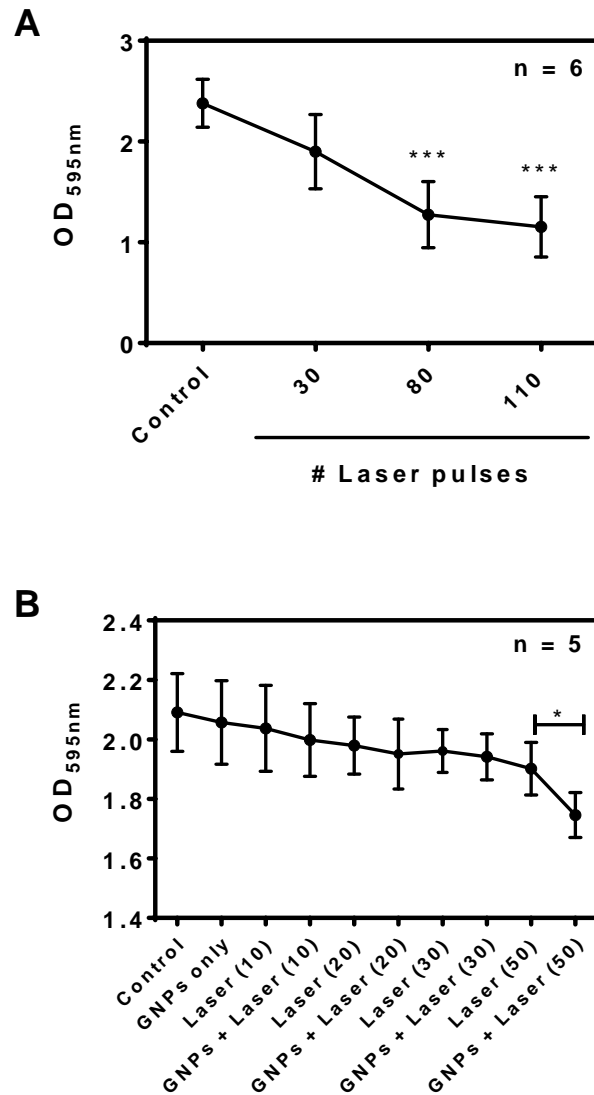


Figure 3: Lower threshold of laser dosage required to destroy MRSA biofilms. MRSA biofilms were grown for 24 h then exposed to A) laser alone or B) GNPs at 62.5 $\mu\text{g/mL}$ followed by laser irradiation (values in parentheses indicate number of laser pulses). A) CV assay results from biofilms treated with laser alone show a significant reduction in biofilm biomass after exposure to 80 or 110 laser pulses, but no significant reduction in biomass after exposure to 30 pulses compared to controls. B) CV assay results show significant reduction of biomass after treatment of biofilms with GNPs and 50 laser pulses. Data in both graphs are shown as the mean \pm SD. Statistical significance was calculated using one-way ANOVA followed by Tukey multiple comparison tests and is denoted by *** $p < 0.001$ compared to controls and * $p < 0.05$.

Figure 4

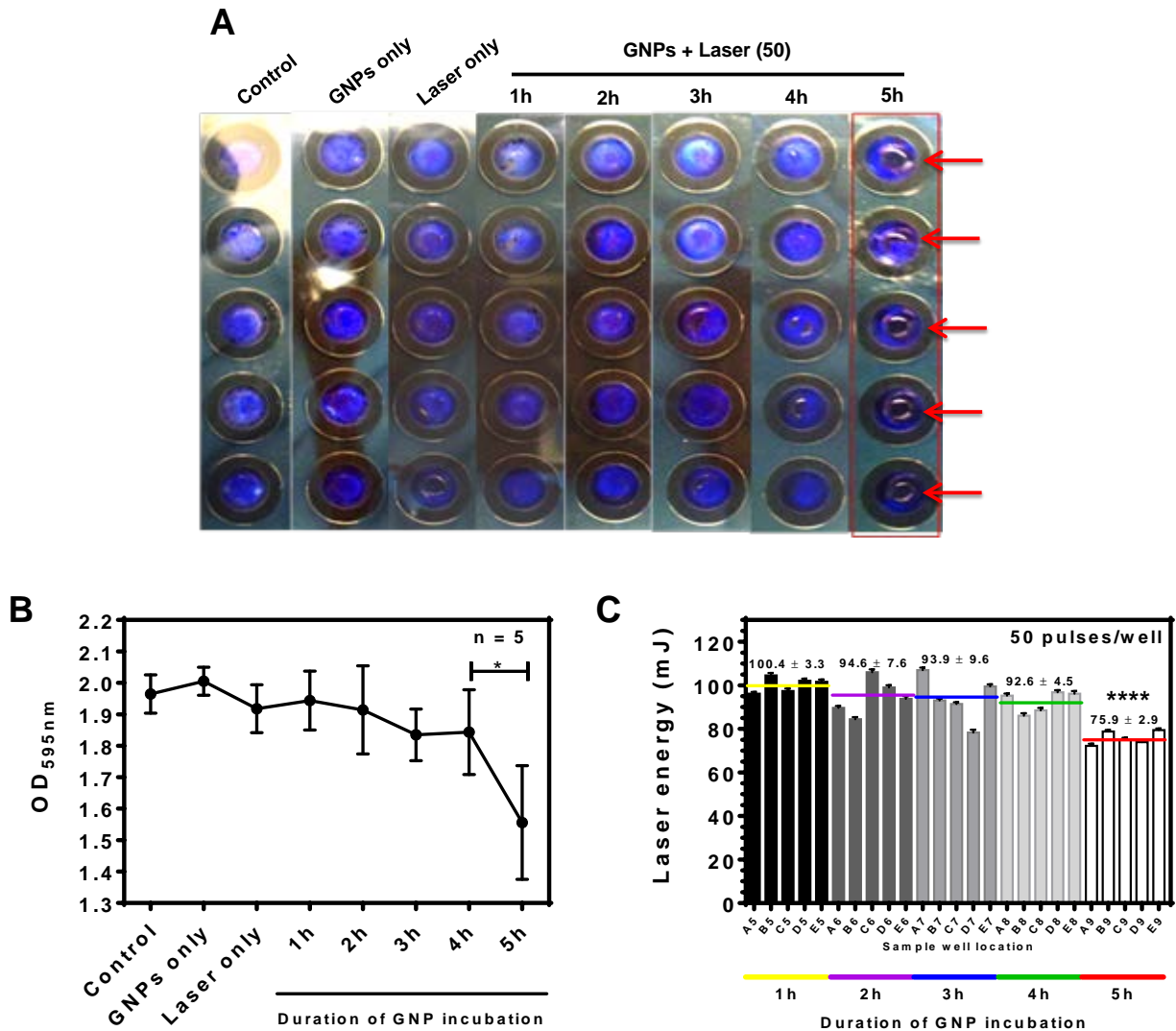


Figure 4: Duration of nanoparticle incubation needed to achieve optimal GNP-assisted laser therapy-induced destruction of MRSA biofilms. A) Images of biofilms treated with 125 $\mu\text{g/mL}$ GNPs for 1 to 5 h prior to exposure to 50 laser pulses show maximal destruction when biofilms are treated with GNPs for 5 h. Dark areas in the center of the wells indicate regions of biofilm dispersion (red arrows). B) Corresponding CV absorbance measurements show significant reduction in biomass for 5 h of GNP incubation prior to laser treatment. C) Power meter readings show that the laser pulse energy passing through individual wells of the sample plate were significantly lower for the 5 h time-point compared to the other time-points, suggesting the energy absorption was highest in biofilms treated with GNPs for 5 h. Colored lines represent the calculated mean value of the average pulse energy for the 5 wells in each treatment group. Data in both graphs are shown as the mean \pm SD. Statistical significance was calculated using one-way ANOVA followed by a Tukey multiple comparison tests and is denoted by $*p < 0.05$ and $****p < 0.0001$ for the 5 h group compared to the other treatment groups.

Figure 5

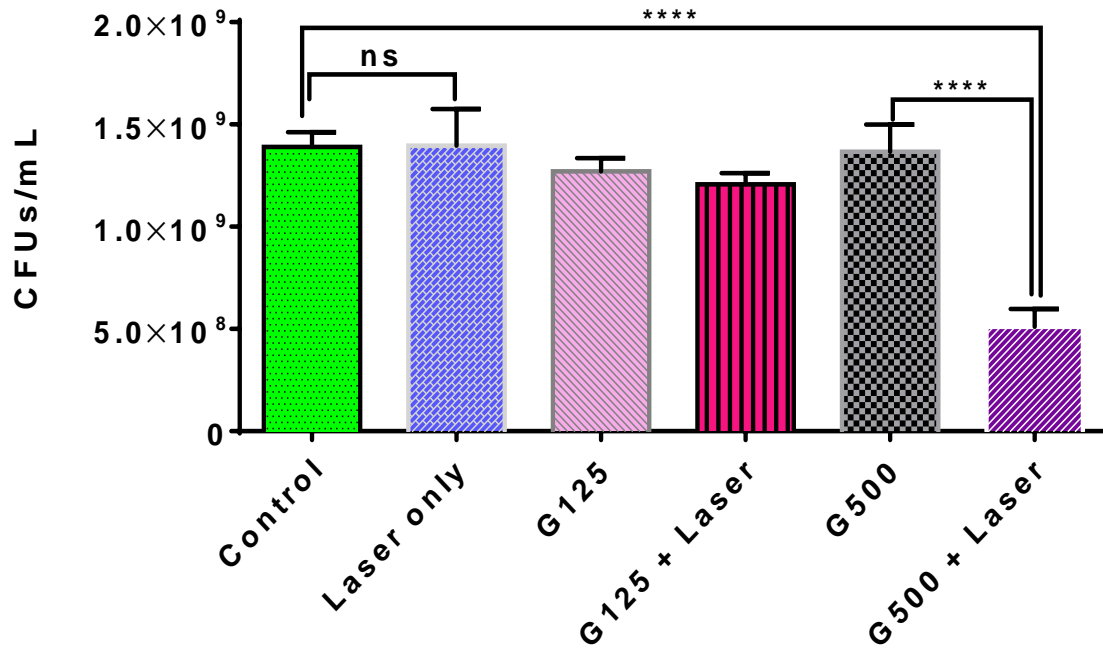


Figure 5: CFU assays revealed that combination therapy of GNPs plus laser treatment dispersed MRSA bacterial colonies from biofilms. Treatment of biofilms with 500 $\mu\text{g/mL}$ of GNPs (G500) followed by 50 laser pulses caused a $63 \pm 8\%$ reduction in bacterial colonies, whereas use of 125 $\mu\text{g/mL}$ of GNPs (G125) with 50 laser pulses did not cause a decrease in biofilm colonies compared to controls. Data are shown as the mean \pm SD of three independent experiments with $n = 3$ samples per treatment group. Statistical significance was calculated using one-way ANOVA with a post hoc Tukey multiple comparison tests and is denoted by **** $p < 0.0001$.

Figure 6

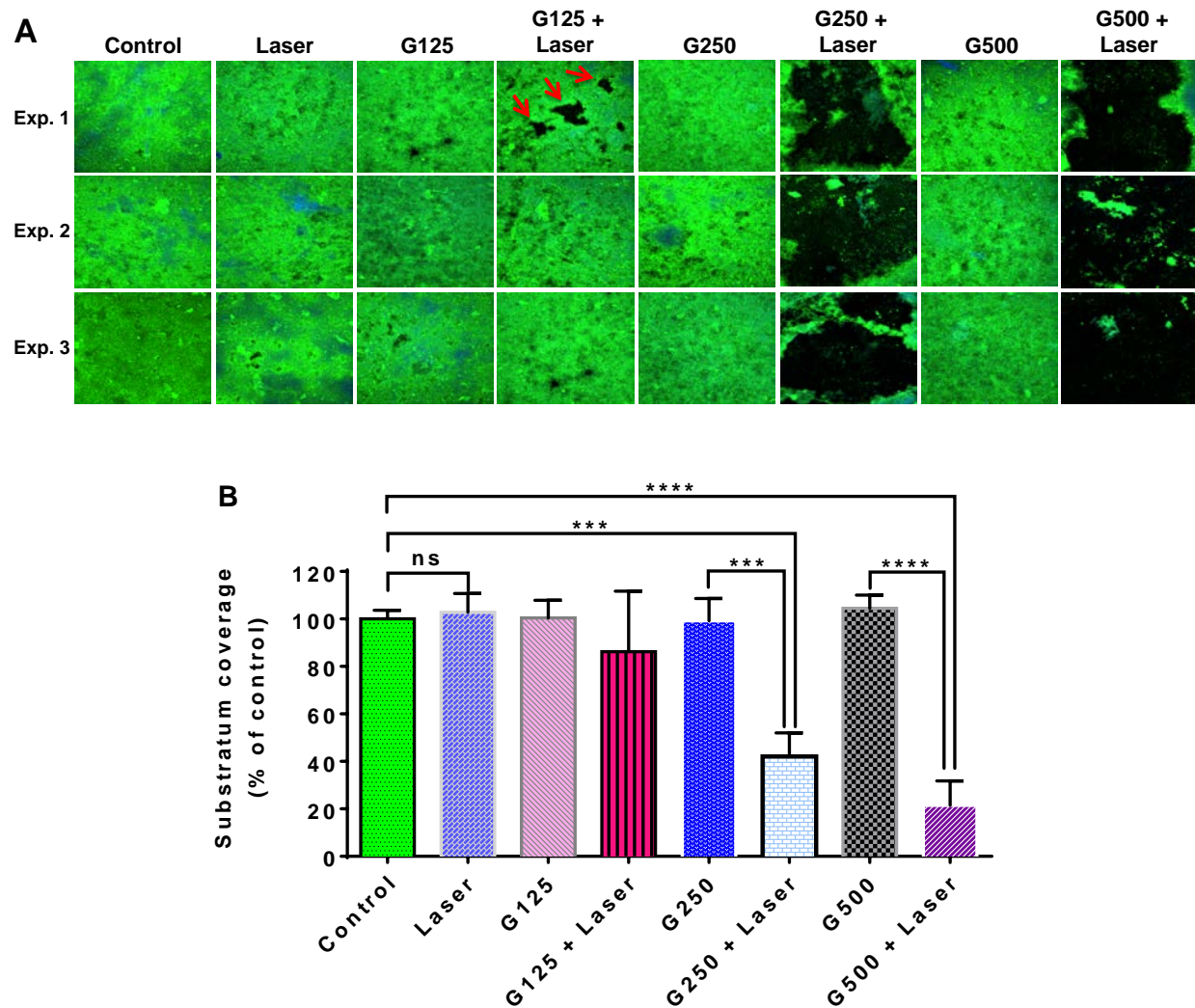


Figure 6: Confocal microscopy revealed extensive damage in MRSA biofilms treated with GNP-assisted laser therapy. A) Representative confocal micrographs of biofilms stained with Con-A (polysaccharide; green) and DAPI (nucleic acids; blue) after treatment. Treatment with 50 laser pulses alone or GNPs alone at 125, 250 or 500 $\mu\text{g/mL}$ caused no visible damage to the biofilms. Use of GNPs at 125 $\mu\text{g/mL}$ (G125) plus laser exposure had a slight effect in some of the samples (red arrows), while GNPs at 250 (G250) or 500 $\mu\text{g/mL}$ (G500) plus laser exposure caused obvious biofilm dispersion. B) Graph shows confocal microscopy image analysis data represented as the mean \pm SD of three independent experiments with $n = 3$ samples per treatment group and 5 FOVs captured per sample. Results reveal that use of 500 $\mu\text{g/mL}$ of GNPs plus laser irradiation led to the highest biofilm dispersion. Statistical significance was calculated using one-way ANOVA followed by Tukey multiple comparison tests and is denoted by *** $p < 0.001$ and **** $p < 0.0001$.

8. REFERENCES

1. Coggan, K.A., *Nitric oxide is bactericidal to the ESKAPE pathogens: Time for a radical approach*. Retrieved from http://www.novantherapeutics.com/files/3713/7398/8986/bactericidal_nitric_oxide.pdf, 2013.
2. *Antibiotic resistance threats in the United States, 2013*. Centers for Disease Control and Prevention: Retrieved from <http://www.cdc.gov/drugresistance/threat-report-2013/pdf/ar-threats-2013-508.pdf>.
3. Roy, D.C., et al., *Ciprofloxacin-loaded keratin hydrogels prevent Pseudomonas aeruginosa infection and support healing in a porcine full-thickness excisional wound*. Adv Wound Care (New Rochelle), 2015, **4**(8): p. 457-68.
4. Robson, M.C., *Wound infection: A failure of wound healing caused by an imbalance of bacteria*. Surg Clin North Am, 1997, **77**(3): p. 637-50.
5. Boucher, H.W., et al., *Bad bugs, no drugs: No ESKAPE! An update from the Infectious Diseases Society of America*. Clin Infect Dis, 2009, **48**(1): p. 1-12.
6. Sutter, D.E., et al., *High incidence of multidrug-resistant gram-negative bacteria recovered from Afghan patients at a deployed US military hospital*. Infect Control Hosp Epidemiol, 2011, **32**(9): p. 854-60.
7. Keen III, E.F., et al., *Incidence and bacteriology of burn infections at a military burn center*. Burns, 2010, **36**(4): p. 461-8.
8. Arias, C.A. and B.E. Murray, *Antibiotic-resistant bugs in the 21st century — A clinical super-challenge*. N Engl J Med, 2009, **360**(5): p. 439-43.
9. Rice, L.B., *Federal funding for the study of antimicrobial resistance in nosocomial pathogens: No ESKAPE*. J Infect Dis, 2008, **197**(8): p. 1079-81.
10. Costerton, J.W., et al., *Mechanism of electrical enhancement of efficacy of antibiotics in killing biofilm bacteria*. Antimicrob Agents Chemother, 1994, **38**(12): p. 2803-9.
11. Costerton, J.W., et al., *How bacteria stick*. Sci Am, 1978, **238**(1): p. 86-95.
12. Stewart, P.S., *Mechanisms of antibiotic resistance in bacterial biofilms*. Int J Med Microbiol, 2002, **292**(2): p. 107-13.
13. Hall-Stoodley, L., et al., *Bacterial biofilms: from the natural environment to infectious diseases*. Nat Rev Microbiol, 2004, **2**(2): p. 95-108.
14. Feldman, M., et al., *Therapeutic potential of thiazolidinedione-8 as an antibiofilm agent against Candida albicans*. PLoS ONE, 2014, **9**(5): p. e93225.
15. Beloin, C., et al., *Novel approaches to combat bacterial biofilms*. Curr Opin Pharmacol, 2014, **18**(0): p. 61-8.
16. Blackledge, M.S., et al., *Biologically inspired strategies for combating bacterial biofilms*. Curr Opin Pharmacol, 2013, **13**(5): p. 699-706.
17. Millenbaugh, N.J., et al., *Photothermal killing of Staphylococcus aureus using antibody-targeted gold nanoparticles*. Int J Nanomedicine, 2015, **10**: p. 1953-60.
18. Kojic, N., et al., *Focal infection treatment using laser-mediated heating of injectable silk hydrogels with gold nanoparticles*. Adv Function Mater, 2012, **22**(18): p. 3793-8.
19. Zharov, V.P., et al., *Photothermal Nanotherapeutics and Nanodiagnostics for Selective Killing of Bacteria Targeted with Gold Nanoparticles*. Biophys J, 2006, **90**(2): p. 619-27.
20. Lukianova-Hleb, E., et al., *Plasmonic nanobubbles as transient vapor nanobubbles generated around plasmonic nanoparticles*. ACS Nano, 2010, **4**(4): p. 2109-23.

21. Norman, R.S., et al., *Targeted photothermal lysis of the pathogenic bacteria, Pseudomonas aeruginosa, with gold nanorods*. Nano Lett, 2007, **8**(1): p. 302-6.
22. Meeker, D.G., et al., *Synergistic photothermal and antibiotic killing of biofilm-associated Staphylococcus aureus using targeted antibiotic-loaded gold nanoconstructs*. ACS Infect Dis, 2016, **2**: p. 241-50.
23. Lee, S.-M., et al., *Targeted chemo-photothermal treatments of rheumatoid arthritis using gold half-shell multifunctional nanoparticles*. ACS Nano, 2013, **7**(1): p. 50-7.
24. Kirui, D., et al., *Tumor vascular permeabilization using localized mild hyperthermia to improve macromolecule transport*. Nanomedicine: NBM, 2014, **10**(7): p. 1487-96.
25. Krishnan, S., et al., *Nanoparticle-mediated thermal therapy: Evolving strategies for prostate cancer therapy*. Intl J Hyperthermia, 2010, **26**(8): p. 775-89.
26. Kharkwal, G.B., et al., *Photodynamic therapy for infections: clinical applications*. Lasers Surg Med, 2011, **43**(7): p. 755-67.
27. Erin, B.D., et al., *Gold nanorod assisted near-infrared plasmonic photothermal therapy (PPTT) of squamous cell carcinoma in mice*. Cancer Lett, 2008, **269**(1): p. 57-66.
28. Mocan, L., et al., *Surface plasmon resonance-induced photoactivation of gold nanoparticles as bactericidal agents against methicillin-resistant Staphylococcus aureus*. Int J Nanomedicine, 2014, **9**: p. 1453-61.
29. Jain, P., et al., *Review of some interesting surface plasmon resonance-enhanced properties of noble metal nanoparticles and their applications to biosystems*. Plasmonics, 2007, **2**(3): p. 107-18.
30. Jain, P.K., et al., *Calculated absorption and scattering properties of gold nanoparticles of different size, shape, and composition: Applications in biological imaging and biomedicine*. J Phys Chem B, 2006, **110**(14): p. 7238-48.
31. El-Sayed, I.H., et al., *Surface plasmon resonance scattering and absorption of anti-EGFR antibody conjugated gold nanoparticles in cancer diagnostics: Applications in oral cancer*. Nano Lett, 2005, **5**(5): p. 829-34.
32. Link, S. and M.A. El-Sayed, *Optical properties and ultrafast dynamics of metallic nanocrystals*. Ann Rev Phys Chem, 2003, **54**(1): p. 331-66.
33. Kim, J.-W., et al., *Photothermal antimicrobial nanotherapy and nanodiagnostics with self-assembling carbon nanotube clusters*. Lasers Surg Med, 2007, **39**(7): p. 622-34.
34. Chen, C.-W., et al., *Metal nanobullets for multidrug resistant bacteria and biofilms*. Adv Drug Del Rev, 2014, **78**(0): p. 88-104.
35. Dai, X., et al., *Multifunctional nanoplatfoms for targeted multidrug-resistant-bacteria theranostic applications*. ACS Appl Mater Interf, 2013, **5**(21): p. 11348-54.
36. Kuo, W.S., et al., *Biocompatible bacteria@Au composites for application in the photothermal destruction of cancer cells*. Chem Commun, 2008: p. 4430-32.
37. Archer, N.K., et al., *Staphylococcus aureus biofilms: Properties, regulation and roles in human disease*. Virulence, 2011, **2**(5): p. 445-59.
38. Vento, T.J., et al., *Staphylococcus aureus colonization of healthy military service members in the United States and Afghanistan*. BMC Infect Dis, 2013, **13**(1): p. 325.
39. Periasamy, S., et al., *How Staphylococcus aureus biofilms develop their characteristic structure*. Proc Natl Acad Sci USA, 2012, **109**(4): p. 1281-6.
40. Akers, K.S., et al., *Biofilms and persistent wound infections in United States military trauma patients: a case-control analysis*. BMC Infect Dis, 2014, **14**: p. 190.

REPORT DOCUMENTATION PAGE

The public reporting burden for this collection of information is estimated to average 1 hour per response, including the time for reviewing instructions, searching existing data sources, gathering and maintaining the data needed, and completing and reviewing the collection of information. Send comments regarding this burden estimate or any other aspect of this collection of information, including suggestions for reducing the burden, to Washington Headquarters Services, Directorate for Information Operations and Reports, 1215 Jefferson Davis Highway, Suite 1204, Arlington, VA 22202-4302, Respondents should be aware that notwithstanding any other provision of law, no person shall be subject to any penalty for failing to comply with a collection of information if it does not display a currently valid OMB Control number. **PLEASE DO NOT RETURN YOUR FORM TO THE ABOVE ADDRESS.**

1. REPORT DATE (DD MM YY) 28 11 16		2. REPORT TYPE Technical Report		3. DATES COVERED (from – to) April 2015 — October 2016	
4. TITLE Gold Nanoparticle-assisted Laser Therapy for the Disruption of Methicillin-resistant <i>Staphylococcus aureus</i> Biofilms				5a. Contract Number: 5b. Grant Number: 5c. Program Element Number: 5d. Project Number: 5e. Task Number: 5f. Work Unit Number: G1025	
6. AUTHORS Dickson Kirui, Ph.D., Tarea Burton, M.S., Gregor Weber, Ph.D., Nancy Millenbaugh, Ph.D.					
7. PERFORMING ORGANIZATION NAME(S) AND ADDRESS(ES) Naval Medical Research Unit San Antonio 3650 Chambers Pass, Bldg. 3610 Joint Base San Antonio-Ft. Sam Houston, TX 78234-6315					
9. SPONSORING/MONITORING AGENCY NAMES(S) AND ADDRESS(ES) BUMED Core Program / Advanced Medical Development Program Office 503 Robert Grant Ave., Bldg. 500 Silver Spring, MD 20910				8. PERFORMING ORGANIZATION REPORT NUMBER Report No. NAMRU-SA-2017-16	
				10. SPONSOR/MONITOR'S ACRONYM(S) BUMED	
				11. SPONSOR/MONITOR'S REPORT NUMBER(s)	
12. DISTRIBUTION/AVAILABILITY STATEMENT Approved for public release; distribution is unlimited.					
13. SUPPLEMENTARY NOTES N/A					
14. ABSTRACT <p>The purpose of this study was to develop a method to destroy bacterial biofilms using energy absorbing gold nanoparticles (GNPs) in combination with pulsed laser irradiation. Methicillin-resistant <i>Staphylococcus aureus</i> (MRSA) biofilms were cultured <i>in vitro</i> for 24 hours and then treated with 0, 62.5, 125, 250, or 500 µg/mL of GNPs for 1 to 5 hours. Biofilms were then exposed to 10 to 110 laser pulses (532 nm, 8 ns, 1 Hz) or sham exposed. The crystal violet assay for biofilm biomass revealed that optimal dispersion of MRSA biofilms was achieved after treatment with 500 µg/mL of GNPs for 5 h followed by 50 laser pulses. Treatment of the biofilms with a combination of GNPs and laser irradiation led to a $63 \pm 8\%$ reduction in colony forming units (CFUs) relative to controls and a $79 \pm 10\%$ dispersion of biofilms as evidenced by confocal microscopy. Conversely, biofilms treated with 50 laser pulses alone or GNPs alone showed no discernible dispersion or reduction in CFUs compared to untreated controls. These results demonstrate the use of GNP-assisted laser therapy as a potential strategy to disrupt biofilms and, therefore, enhance the therapeutic efficacy of mainstay antibiotic regimens.</p>					
15. SUBJECT TERMS Biofilm, Infection, Methicillin-resistant <i>Staphylococcus aureus</i> , Gold nanoparticles, Laser, Photothermal					
16. SECURITY CLASSIFICATION OF:			17. LIMITATION OF ABSTRACT UNCL	18. NUMBER OF PAGES 27	19a. NAME OF RESPONSIBLE PERSON CAPT Elizabeth Montcalm-Smith, Ph.D., MSC, USN
a. REPORT UNCL	b. ABSTRACT UNCL	c. THIS PAGE UNCL			19b. TELEPHONE NUMBER (INCLUDING AREA CODE) COMM/DSN: 210-539-5334 (DSN: 389)